Comparison of Structural and Optical Properties Of The Undoped, Zn and Fe Doped PbS Nanocrystalline Films

[1]Bhaskar Jyoti Baruah,
[1] Department of Physics, D. R. College, Golaghat, Assam, India -785621

Abstract: This study has been undertaken to determine the structural and optical properties of undoped and doped PbS films prepared by CBD method. Zn and Fe have been chosen as dopant. Structural properties are studied by SEM and XRD while the optical absorbance, transmittance and reflectance are studied by UV-Visible spectrophotometer. From the XRD data, crystallite size, lattice constant, microstrain and dislocation density and from the optical data, direct and indirect band gaps of the films have been determined.

1. Introduction:

PbS is a IV-VI semiconductor crystallizing in the rocksalt structure (fcc) with lattice constant 5.936 Å. The small effective masses and large dielectric constant gives it a higher values of exciton Bohr radius (~ 20 nm) in comparison to CdSe (~5.4 nm) [1] and CdS (~2.8 nm) [2] . Therefore strong quantum confinement can be easily assessed in PbS.

Nanocrystalline films of PbS have been prepared basically by the Chemical Bath Deposition (CBD) method. This method is simple, inexpensive, capable of producing large area, thin and well-adhered films, large number of substrates can be coated in a single run and doping agents can be easily inserted.

An important factor having significant impact on the optoelectronic properties of a thin film is injection of impurities or doping of the films. How various kinds of dopants influence the band gaps and electrical properties of PbS nanocrystalline films have been discussed in the literature [3-15]. There are a few scientific articles discussing Zn and Fe doping in PbS thin film. Joshi et.al [11] observed that the optical band gap of $Pb_{1-x}Fe_xS$ varied from 2.65 to 2.22 eV with the increase of x. Ravishankar et.al [12] studied the optical and magnetic properties of Fe^{2+} doped PbS thin film. They obtained that Fe^{2+} doping decreases the crystallite size, blueshifts the band gap and improves magnetic property Ravishankar and Balu [13] observed that Zn doping enhances optical and electrical properties of the PbS film. Touati et.al [14] observed that Zn doping enhances the applicability of the PbS in solar cell as absorber. Yousefi et.al [15] observed that Zn doping increases the band gap of the PbS film. In this article, the structural and optical properties of undoped and Zn doped nanocrystalline PbS films have been investigated and how Zn doping affects these properties have been discussed . We prepared undoped and doped PbS films by CBD method in a way independent of the above cited works. For instance, we choose the concentration ratio of the sources of Pb, S and the dopant element as 1:2:2 which is different from corresponding ratios in the reported works [11-15]. Also we are using triethanolamine as complexing agent. Our results are expected to be different.

2. Experimental Details:

(a) Deposition of Films

To 5 ml of 0.5 M $Pb(NO_3)_2$ solution in deionized water, 2 ml of 1.5 M triethanolamine (TEA) has been added and the mixture was stirred for 10 minutes. After 10 minutes, while continuing stirring, 4 M NaOH solution was added dropwise until the mixture became transparent. The measurement of pH returned the value 13. We prepared five such baths. In each of the four out of these five baths, we added 3 ml $ZnCl_2$, 6 ml $ZnCl_2$, 3 ml $FeCl_3$ and 6 ml $FeCl_3$ solutions respectively. The concentrations of $ZnCl_2$ and $FeCl_3$ solutions were 1M. The fifth bath was left without addition of impurity ($ZnCl_2$ or $FeCl_3$). After addition of $ZnCl_2$, a few white coloured coloidal particles of $Zn(OH)_2$ became visible. Similarly, on addition of $FeCl_3$, large homogeneous precipitation of $Fe(OH)_3$ occured. Again the mixtures were stirred for 10 minutes. After inserting chemically and ultrasonically cleaned glass substrates into the baths, 6 ml of 1M thiourea was added and the baths were topped up with deionized water to make the total volume of 100 ml. The reactions were allowed to take place at room temperature (28°C). After 3 hours, the substrates were removed from the baths. We did not get any film from the baths where 6 ml of $FeCl_3$ and $ZnCl_2$ were added and hence the substrates from these baths were not considered for characterization. The films from the remaining baths were washed with doubly distilled water, dried in air and stored in vacuum desicator with silica gel. The undoped film has been coded as 'PbS/Undoped', Zn doped as 'PbS/Zn' and Fe doped as 'PbS/Fe'. The sides facing the walls of the bath were considered suitable for characterizations.

(b) Characterization of the Films

The X-ray diffraction pattern of the films were recorded by Bruker AXS D8 Advance diffractometer at room temperature with CuKα radiation having wavelength 1.5406 Å and Si(Li) PSD detector. The surface morphology was studied by JEOL JSM - 6390LV Scanning Electron Microscope. The optical absorbance, transmittance and reflectance were measured by Varian, Cary 5000 spectrophotometer with wavelength accuracy ±0.1 nm (UV–Vis), ±0.4 nm (NIR) and limiting resolution 0.05 nm (UV–Vis), 0.2 nm (NIR).

3. Results and Discussion:

3.1 Surface Morphology:

The surface morphology of the 'PbS/Undoped', 'PbS/Zn' and 'PbS/Fe' films are shown in Fig.1(a)-(c). It is observed from these figures that the 'PbS/Fe' film is thinner than 'PbS/Zn' film which is again thinner than 'PbS/Undoped' film. Also, the coverage on the substrates deteriorate as we move from 'PbS/Undoped' to 'PbS/Zn' to 'PbS/Fe' films. The paricle sizes are found in between 150-350 nm in 'PbS/Undoped', 160-220 nm in 'PbS/Zn' and 190-230 nm in 'PbS/Fe' films. That is, wider size distribution has been observed in the undoped film due to which surface of the 'PbS/Undoped' film seems to be rough .

The thicknesses of the films, as determined by gravimetric method, were measured as 1200, 850 and 480 nm for the films 'PbS/Undoped', 'PbS/Zn' and 'PbS/Fe' respectively. It means that addition of impurity (Zn and Fe) in the bath reduces the thickness of the films and deteriorates the surface coverage, the underlying reason for the same can be explained as below-

When $ZnCl_2$ and $FeCl_3$ were added to the bath containg NaOH, precipitation of $Zn(OH)_2$ (white) and $Fe(OH)_3$ (red brown) occurs via following reactions:

$$ZnCl_2 + 2NaOH \Rightarrow Zn(OH)_2 + 2NaCl$$

$$Fe(Cl)_3 + 3NaOH \Rightarrow Fe(OH)_3 + 3NaCl$$

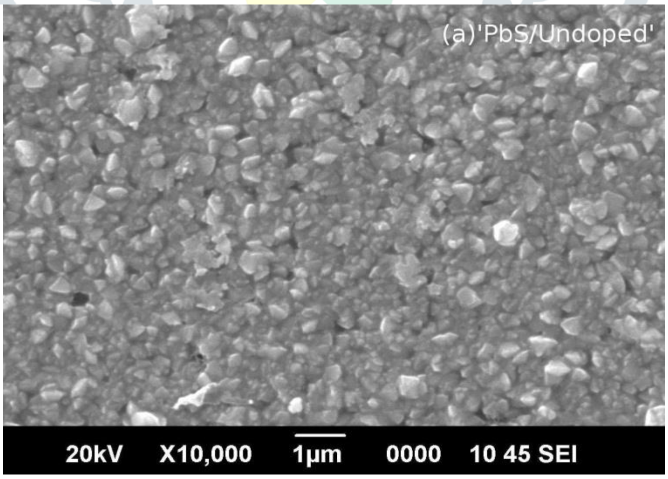

The solubility products of $Pb(OH)_2$, $Zn(OH)_2$ and $Fe(OH)_3$ are 10^{-15} M^3, 10^{-16} M^3 and 10^{-39} M^4 [16] respectively. Since the solubility products of $Zn(OH)_2$ and $Fe(OH)_3$ are lower than that of $Pb(OH)_2$, therefore when solutions of $Zn(Cl)_2$ and $Fe(Cl)_3$ were added in the transparent solutions of $Pb(NO_3)_2$, homogeneous precipitations of $Zn(OH)_2$ and $Fe(OH)_3$ occurs . $Fe(OH)_3$ precipitates in large amount owing to very low solubility product. Due to these precipitations, the number of OH^-s available for decomposition of thiourea has been reduced. Consequently, the reaction rate slows down and fewer ions reach the surface giving rise to thinner films. When the volume of the $ZnCl_2$ and $FeCl_3$ has been doubled (6 ml), the homogeneous precipitation became so dominant that no film formed on the substrate. While preparing Bi doped PbS film, Pentia et.al [3] also observed that no film had been deposited on the substrate when the volume of the $Bi(NO_3)_3$ added to the bath reached 5 ml. They put forwarded same argument in favour of not getting the film.

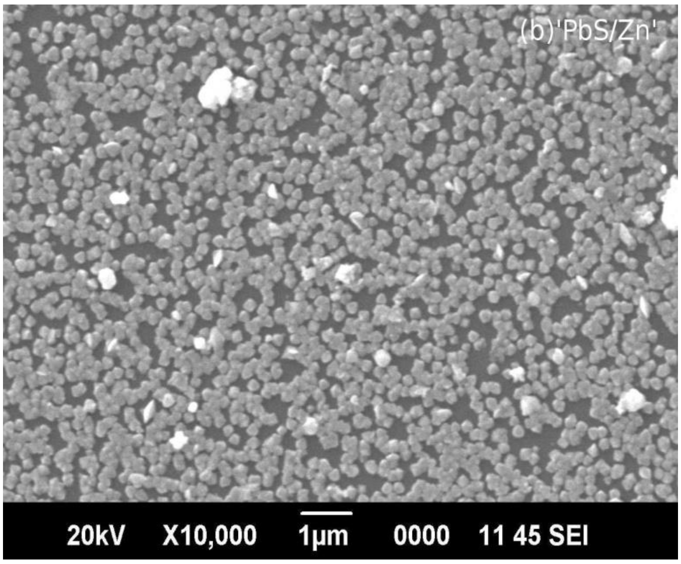

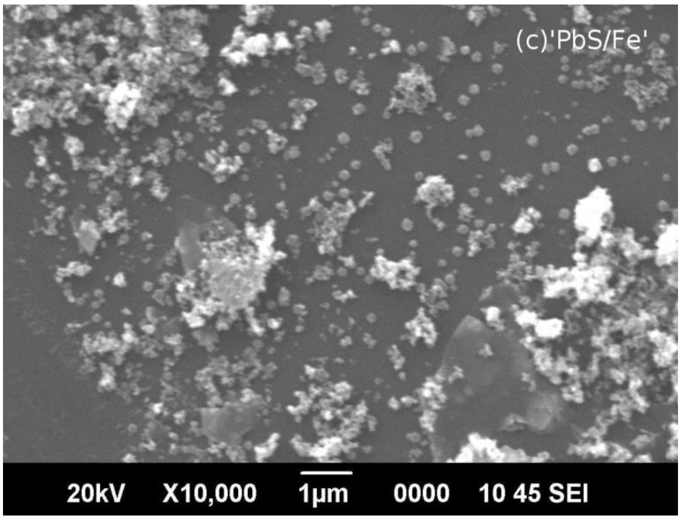

Fig.1: SEM image of (a) 'PbS/Undoped', (b) 'PbS/Zn' film, (c) 'PbS/Fe' films

3.2 Structural Properties

The XRD patterns [Fig.2] confirmed the formation of fcc structured PbS phase [ICDD card no.78-1900] in all the films. The 'PbS/Undoped' film is (200) oriented. The growth preference of the crystallites shift towards (111) in the doped films. It is observed that the (111) plane becomes the most preferred plane of growth for the crystals in Zn doped film. Similar observations were reported by Rajashree et.al [17] for Ni doped PbS thin film. The intensity ratio I_{200}/I_{111} are 1.39, 1.12 and 0.76 for the 'PbS/Undoped', 'PbS/Fe' and 'PbS/Zn' films respectively.

The peak positions of the doped films are shifted in comparison to the undoped film. This shift is more prominent in the 'PbS/Fe' film. The shift in the peak positions is due to the increase in defects in the doped films. This is supported by the larger values of strain in the doped films (Table 1). Broadening of the XRD peaks indicate that the crystallites of the doped films are smaller than the undoped film. The Debye-Scherrer formula returns the crystallite size as 32, 28 and 22 nm for the 'PbS/Undoped', 'PbS/Zn' and 'PbS/Fe' films respectively.

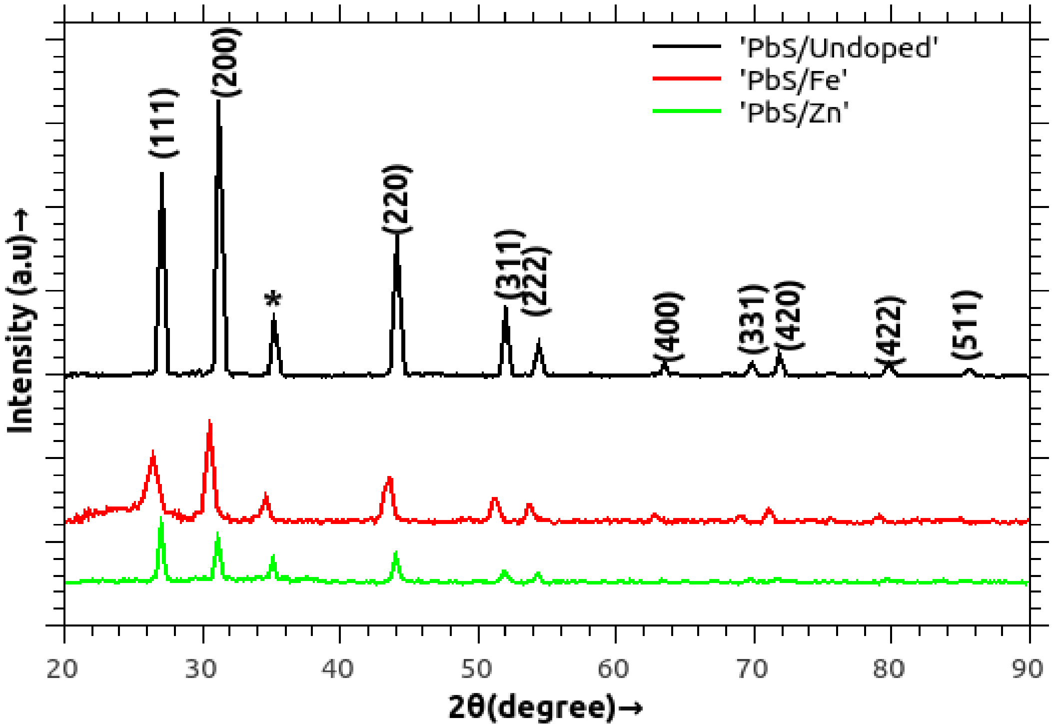

Fig.2: XRD pattern of the films

The lattice constants are evaluated as 5.935, 5.942 and 5.955Å for the 'PbS/Undoped', 'PbS/Zn', 'PbS/Fe' films respectively from the Nelson- Riley plot [Fig.3]. We noticed lattice expansion on doping (bulk value of lattice constant of PbS =5.936 Å) which is unusual. As the ionic radii of both Zn^{2+} (0.74Å) and Fe^{3+} (0.64Å) are smaller than that of Pb^{2+} (1.20Å), there should have been lattice contraction had Zn^{2+} and Fe^{3+} substituted Pb^{2+}. There are some reports on lattice expansions in case of doping by smaller atoms. Nayak et. al [18] observed lattice expansion while forming $Pb_{1-x}Cd_xS$ film which they interpreted as PbS entering as interstitial into CdS lattice causing this expansion. Gassoumi et. al [10] observed lattice expansion in Mg doped PbS nanocrystalline film and attributed it to the substitution of Pb and/or S atoms by Mg in the rock salt crystal structure. Rajashree et.al [17] interpreted the lattice expansion in the PbS crystal after incorporation of Ni impurities as occupation of interstitial positions and/or creation of structural vacancies. In another study of Cd doped PbS thin film, the same group [5] attributed lattice expansion to the ionic radii mismatch between Pb^{2+} and Cd^{2+}.

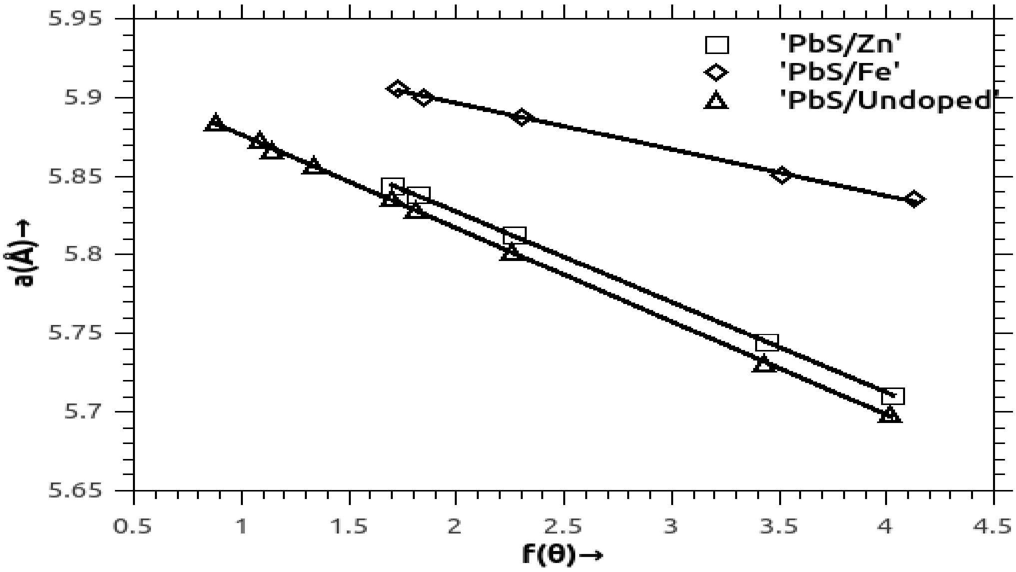

Fig. 3: Nelson-Riley Plot

In the present case, the lattice expansion may be due to the incorporation of Fe and Zn atoms to the interstitial positions [19]. The injected impurities deform the PbS lattice which hampers the grain growth and induces lattice expansion.

We have observed in Fig.2 (XRD pattern) that the intensities of all the XRD peaks of the 'PbS/Zn' and the 'PbS/Fe' films are smaller than the 'PbS/Undoped' film implying deteriorating crystallinity of the doped films. The microstrain and dislocation density are also found larger in doped films (Table1).

In the XRD pattern (fig.2), a peak (marked *) is observed. This XRD peak is due to oxygen incorporation and nonstoichiometry. In CBD films, sizeable amount of oxygen is found at the surface layer. This is due to the adsorbed oxygen atoms and OH^- ions. The adsorbed OH^- ions form $Pb(OH)_2$ with Pb, in conditions where the solubility product of $Pb(OH)_2$ is not reached in the bulk solution. Although the greatest part of $Pb(OH)_2$ transforms into PbS, a minor part remains as hydroxide or hydrated oxide. In a Pb rich film, a large part of the oxygen content is in the form of PbO and water. On the other hand, in a S rich film, the adsorbed O^{2-} or OH^- ions are in the form of SO_4^{2-} or SO_3^{2-} [3].

3.3 Optical Properties by UV-Vis. Spectrophotometer

(i) Optical Absorbance, Transmittance, Reflectance and Urbach Energy

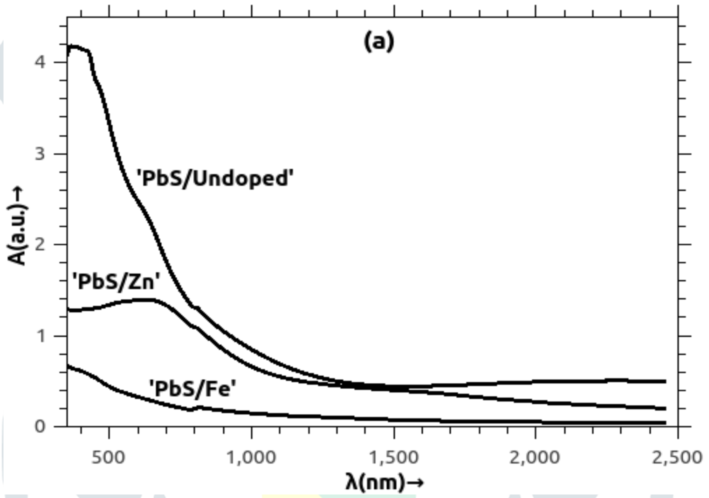

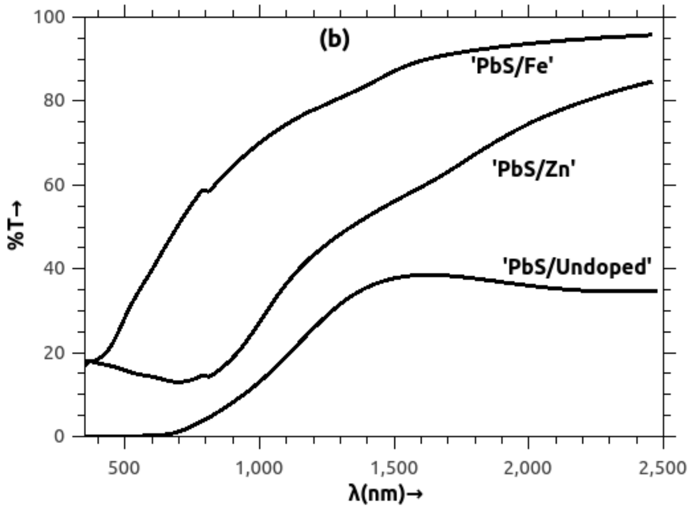

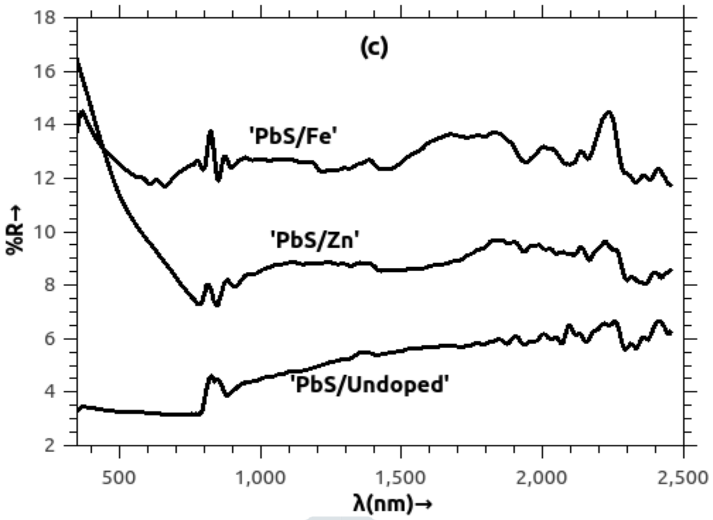

Fig 4: Plot of (a) Absorbance (A), (b) Transmittance (%T) and (c) Reflectance (%R) against wavelength (λ)

The variation of optical absorbance (A), transmittance (T) and reflectance (R) of the films against the wavelength (350-2500 nm) are illustrated in Fig. 4 (a)-(c). Contrary to the bulk PbS which is IR absorber (~3020 nm), these films absorb in the visible [Fig.4(a)]. The effect of thickness comes into play in the absorbances of the films (specially in the visible region) in the sense that thicker films are better absorber. As the 'PbS/Undoped' film has got highest thickness, its absorbance is maximum.Being thinner than the other two, the 'PbS/Fe' film is the least absorbing.

Fig. 4(b) shows that doping enhances the transparency of the films to great extent. Films have shown high transmittance in the NIR region. The maximum transmittance of the 'PbS/Undoped' film is 40% which increased to 85% and 95% for 'PbS/Zn' and 'PbS/Fe' respectively. Thinner films are showing better transparency in the entire wavelength range. The sharp decrease of transmittance towards the visible region indicates fundamental transitions.

The reflectances of the films decrease from 'violet' to 'red' and then tend to remain steady with fluctuations within narrow range [Fig. 4(c)]. The fall of reflectances in the visible region is sharper in the 'PbS/Zn' film (from 16.5% to 7.5%). The 'PbS/Undoped' film has got the least reflectance due to its high absorbance and surface roughness.

The direct band gaps of the films were estimated as 1.55, 1.3 and 2.2 eV for the 'PbS/Undoped', 'PbS/Zn' and 'PbS/Fe' films respectively [Fig.5(a)]. Burstein-Moss Effect (BM) [20] and quantum confinement may play into the band gap widening of the 'PbS/Fe' film. On the other hand, we observed band gap narrowing in the 'PbS/Zn' film. It may be due to the overlapping perturbations arising from the interstitial Zn^{2+}s. Interstitial Zn^{2+}s behave as donors. These tend to depress the conduction band by virtue of their attractive potential. There are also repulsion of conduction band electrons by Pb vacancy. As the electrons promptly migrate to the undisturbed positions, this repulsion has limited effect on band structure. If the valence band is not shifted as stongly as the conduction band, the net effect is shrinkage of band gap [21].

The direct band gaps of the films were estimated as 1.55, 1.3 and 2.2 eV for the 'PbS/Undoped', 'PbS/Zn' and 'PbS/Fe' films respectively [Fig.5(a)]. Burstein-Moss Effect (BM) [20] and quantum confinement may play into the band gap widening of the 'PbS/Fe' film. On the other hand, we observed band gap narrowing in the 'PbS/Zn' film. It may be due to the overlapping perturbations arising from the interstitial Zn^{2+}s. Interstitial Zn^{2+}s behave as donors. These tend to depress the conduction band by virtue of their attractive potential. There are also repulsion of conduction band electrons by Pb vacancy. As the electrons promptly migrate to the undisturbed positions, this repulsion has limited effect on band structure. If the valence band is not shifted as stongly as the conduction band, the net effect is shrinkage of band gap [21].

Fig. 5 (b) demonstrates the indirect band gaps of the films. While it is same for the films 'PbS/Undoped' and 'PbS/Fe' (0.51 eV), but somewhat higher in 'PbS/Zn' (0.6 eV).

Various structural and optical parameters are shown in table 1

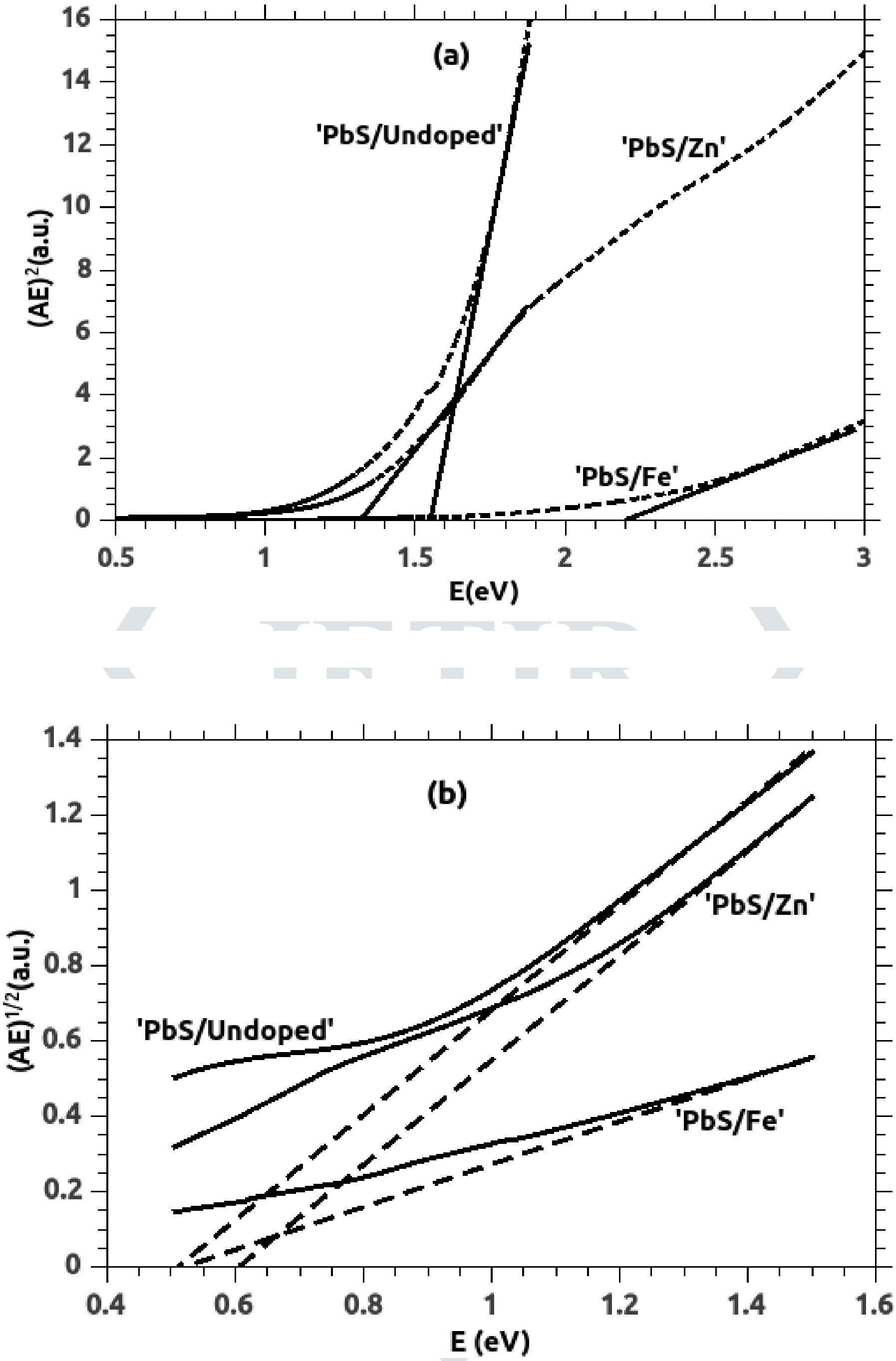

Fig. 5: (a) Direct Band Gaps and (b) Indirect Band Gaps of the Films

Table 1: **Structural and Optical parameters of the films**

Films	D (nm)	a (Å)	ε	ρ(x10^{11}) (cm^{-2})	E_g (eV) (Direct)	E_g (eV) (Indirect)
'PbS/Undoped'	32	5.935	0.0035	2.83	1.55	0.51
'PbS/Fe'	22	5.955	0.0059	9.05	2.2	0.51
'PbS/Zn'	28	5.942	0.0045	4.30	1.3	0.6
D=Crystallite Size; a= Lattice Constant; ε = Microstrain; ρ = Dislocation Density; E_g = Band Gap						

4. Conclusion

(i) Zn and Fe doping deteriorates crystallinity of PbS film by increasing microstrain and dislocation density. The crystallite sizes are smaller in the doped films.

(ii) The doped films exhibit noticeable lattice expansion.

(iii) The undoped film is highly absorbing and less reflecting. Fe and Zn doping enhances the transparency of the films specially in the NIR region.

(iv) The undoped film has direct band gap of 1.55 eV. We notice shrinkage of direct band gap in the Zn doped film (1.3 eV) and widening of the same in the Fe doped film (2.2 eV). The films possess indirect band gap also.

Acknowledgement:

This article is a part of my Ph.D thesis submitted to Gauhati University. I am indebted to the department of Instrumentation and USIC, Gauhati University and my supervisor Prof. Kanak Ch. Sarma for providing the opportunity to carry out this research work. I express my gratitude to the STIC, CUSAT for providing XRD, SEM and UV-Visible-NIR spectrophotometer facilities,

References

1. H. Maoet al., *Physica E* 27 (2005)124
2. Titova et.al, https://arxiv.org/pdf/cond-mat/0606427.pdf
3. Pentia et.al, *Thin Solid Films* 434 (2003) 162
4. Das, Kumar, *Materials Research Bulletin* 47 (2012) 239
5. C. Rajashree, A. R. Balu, V. S. Nagarethinam, *Surface Engineering* 31 (2015) 316
6. S. Thangavel et.al *Thin Solid Films* 520 (2012) 5206
7. Zheng et.al, *Materials Letters* 167 (2016) 128
8. R. Sakthi Sudar Saravanan et.al, *Journal of Alloys and Compounds* 627 (2015) 69
9. N Mathur et.al, *Physica E* 23 (2004) 56
10. A Gassoumi et.al, *Journal of Molecular Structure* 1116 (2016) 67
11. R K Joshi et.al, *Nanotechnology* 14 (2003) 809
12. S.Ravishankar et.al, *Optik - International Journal for Light and Electron Optics* 134 (2017) 121
13. Ravishankar, Balu *Surface Engineering* 33 (2017) 506
14. Touati et.al, *Materials Science in Semiconductor Processing* 34 (2015) 82
15. R Yousefi *et al*, *Chin. Phys. B* 23 (2014) 108101
16. G Hodes, *Chemical Solution Deposition of Semiconductor Films* (Marcel Dekker Inc. 2003)
17. C. Rajashree, A.R. Balu, *Optik* 127 (2016) 8892
18. B. B. Nayak , H. N. Acharya, G. B. Mitra, *Bull. Mater. Sci.*, 3 (1981) 317
19. Kim et.al, *Thin Solid Films* 377-378 (2000) 798
20. Jacques I. Pankove, “Optical Processes in Semiconductors”, (Dover Publications, Inc. 1975)
21. J. I. Pankove, P . Algrain *Physical Review* 126 (1962) 956